ELSEVIER

Chemical Engineering Science 59 (2004) 4999–5008

Chemical Engineering Science

www.elsevier.com/locate/ces

Hydrodynamics and mass transfer in an upflow monolith loop reactor: influence of vibration excitement

C.O. Vandu, J. Ellenberger, R. Krishna*

Van't Hoff Institute for Molecular Sciences, University of Amsterdam, Nieuwe Achtergracht 166, 1018 WV Amsterdam, The Netherlands

Received 9 February 2004; received in revised form 15 June 2004; accepted 4 July 2004
Available online 15 September 2004

Abstract

The hydrodynamics and mass-transfer characteristics of monolith loop reactors, with upflow of gas and liquid phases through the channels, have been investigated and compared with conventional internal airlift reactor and bubble column configurations. The volumetric mass-transfer-coefficient per unit volume of dispersed gas bubbles, k_La/ε_G, is significantly higher for monolith reactors than for airlift and bubble columns. This improvement is due to the superior mass-transfer characteristics of Taylor flow in narrow capillaries. Application of low-frequency vibrations has the effect of significantly improving k_La/ε_G for all reactor configurations studied. For monoliths, vibrations also have the additional beneficial effect of improving the gas–liquid distribution through the channels.

Keywords: Monolith reactors; Gas holdup; Taylor bubbles; Bubble columns; Internal airlift; Mass-transfer coefficient; Vibration excitement

1. Introduction

Monolith loop reactors are used for carrying out a variety of solid catalysed gas–liquid reactions such as hydrogenations and oxidations (Kapteijn et al., 2001; Roy et al., 2004). The main advantages over trickle beds, slurry bubble columns and airlifts are low pressure drop, high mass-transfer rates, and ease of scale-up. Stankiewicz (2001) provides an example of a process for which an in-line monolith reactor is 100 times smaller in size than a conventional reactor and therefore represents a truly intensified process. Most of the published experimental studies relate to *downflow* of both gas and liquid phases in monoliths (Heiszwolf et al., 2001; Kreutzer, 2003; Nijhuis et al., 2001) and very little information is available on *upflow* operation of gas and liquid (Boger et al., 2003). In both upflow and downflow operation of monolith reactors we need to have uniform distribution of gas and liquid phases through the various channels (Heibel et al., 2001).

The first major objective of the present work is to study the hydrodynamics and mass transfer in an *upflow* monolith loop reactor. The second objective is to develop the corresponding data on gas holdup, ε_G, and volumetric mass-transfer coefficient, k_La, also for a bubble column and airlift, using the same column geometry and gas distribution device. The data generated in this work would be useful to the purposes of reactor selection. In earlier studies (Ellenberger and Krishna, 2002, 2003; Krishna and Ellenberger, 2002), we had shown that low-frequency vibrations to the liquid phase can significantly enhance the gas holdup and mass-transfer characteristics of bubble columns. The third objective of the present study is to examine the effect of low-frequency vibrations on the performance of monoliths and airlifts in order to determine to what extent subtle resonance phenomena can improve the performance of these gas–liquid contactors as well.

2. Experimental set-ups

All experiments were carried out in a set-up consisting of a monolith internal loop reactor and a vibration control

* Corresponding author. Tel.: +31-205257007; fax: +31-205255604.
E-mail address: r.krishna@uva.nl (R. Krishna).

0009-2509/$ - see front matter © 2004 Elsevier Ltd. All rights reserved.
doi:10.1016/j.ces.2004.07.089

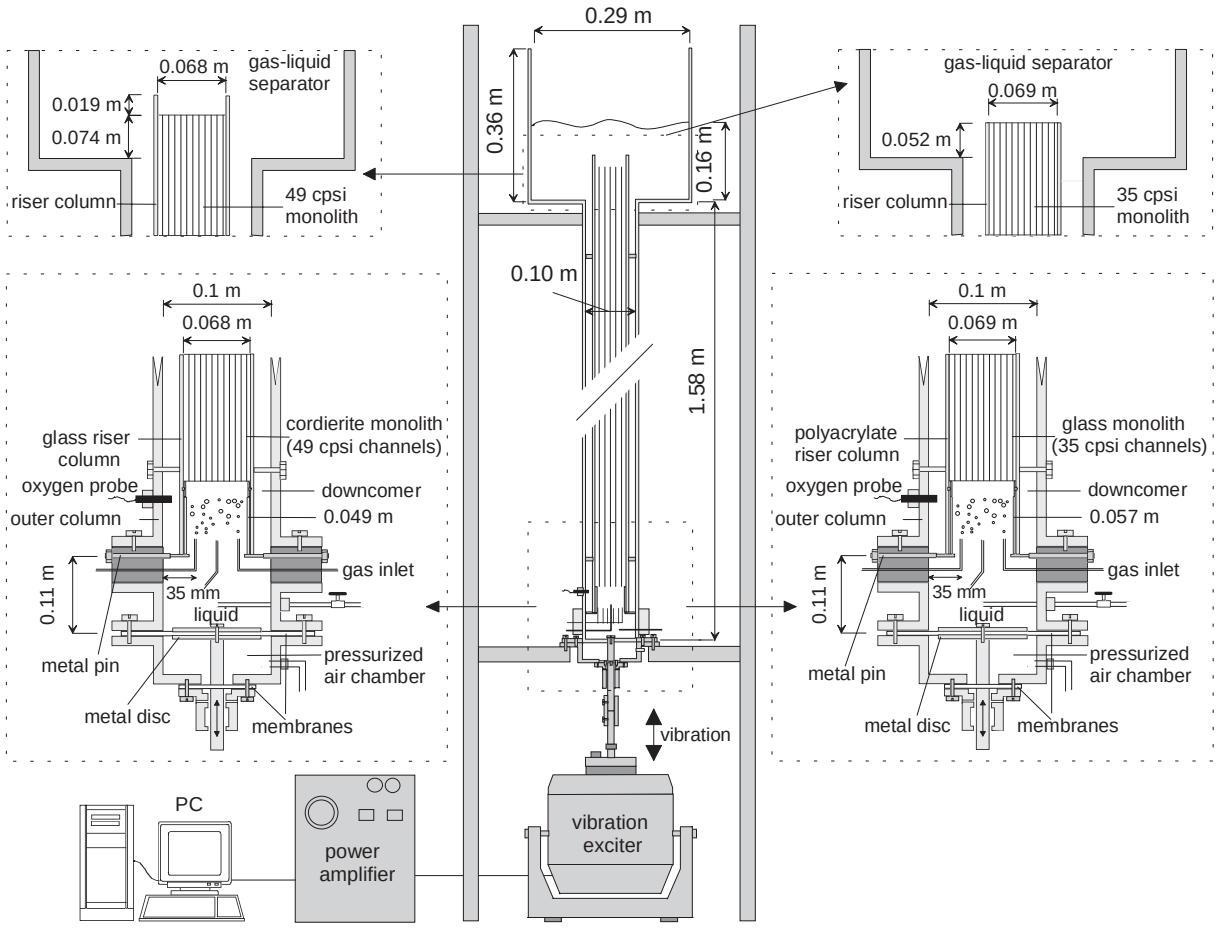

Fig. 1. Experimental set-up for the monolith loop reactors. The set-ups for the airlift and bubble column are derived from the same outer column configuration. For further details of all set-ups visit our website (Vandu et al., 2003).

system. The monolith loop reactor comprises of an outer column, a riser column containing the monolith segments, and a gas–liquid separator unit (see Fig. 1). The outer column and gas–liquid separator were constructed of polyacrylate. The riser column was placed concentrically inside the outer column, the internal diameter of the latter being 0.1 m. Square-channel cordierite and circular-channel glass capillary monoliths were employed. For the square-channel monolith set-up, the riser column was fabricated from glass and had an internal diameter of 0.068 m. On the other hand, the riser column of the circular-channel monolith set-up was made of polyacrylate, with an internal diameter of 0.069 m. The annular space between the riser and outer columns forms the downcomer section of the reactor. The lower end of the riser was supported by means of three metal pins placed at a distance of 0.11 m from the bottom of the reactor. The gas–liquid separator, with an internal diameter of 0.29 m and a height of 0.36 m was mounted at the top of the outer column, a height of 1.58 m from the base of the reactor.

For experiments involving the square-channel monoliths, five identical pieces of cordierite monolith (*Corning GmbH, Germany*), each with 49 cells per square inch (cpsi), were tightly mounted on one another in the 0.068 m diameter glass riser column. Each monolith had square-shaped channels with sides of 3.01 mm and an estimated void fraction of 68.8%. In order to carry out experiments using the circular-channel monoliths, a 1.47 m long monolith tube bundle consisting of 204 circular glass capillaries each with inner and outer diameters of 3 and 4 mm, respectively, was inserted in the 0.069 m diameter polyacrylate riser tube. The capillaries were arranged on a triangular pitch with a pitch distance of 4 mm. The top and bottom of the circular-channel monolith bundle were sealed using a thermoplastic polymer (*Crystalbond 509*, *Printlas Europa*, *The Netherlands*) and the resulting distribution of open channels was 35 cpsi with an estimated void fraction of 38.6% Figs. 2a and b show schematic representations of the circular-channel glass monolith and square-channel cordierite monolith. In this paper, the square- and circular-channel monolith loop reactors are collectively referred to as ‘monolith loop reactors’.

Irrespective of the monolith set-up employed, the bottom of the outer column was sealed by means of a 0.4 mm-thick

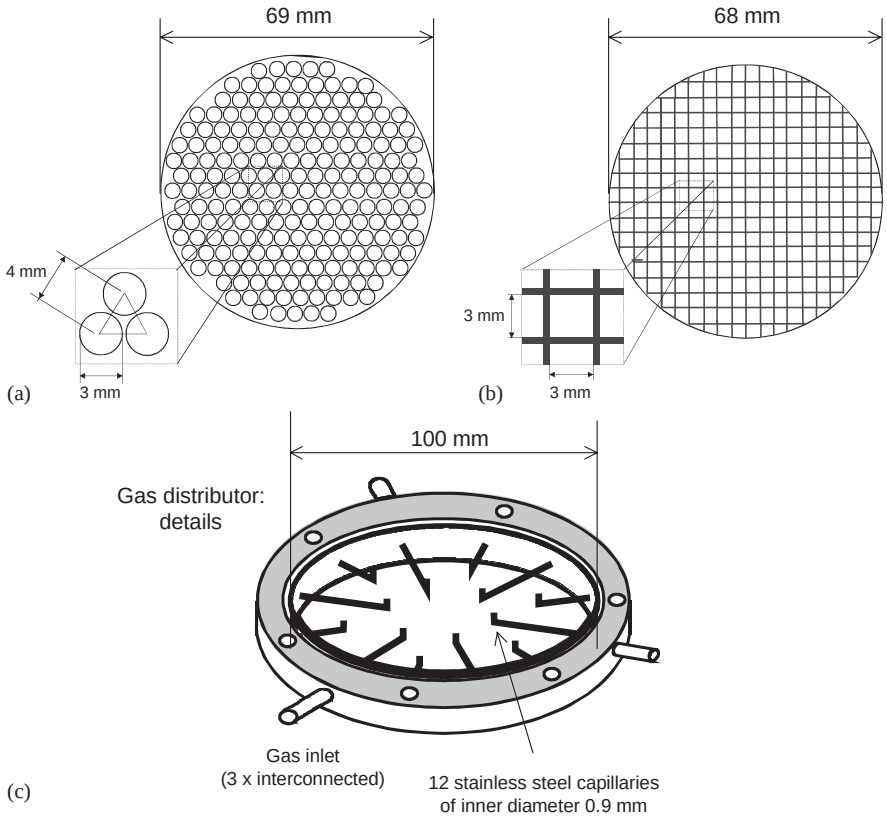

Fig. 2. Schematic representation of (a) the 35 cpsi circular channel glass monolith, (b) the 49 cpsi square-channel cordierite monolith. (c) Details of the gas distribution device. For further details visit our website (Vandu et al., 2003).

silicon rubber membrane tightly sandwiched between two metal discs each with a diameter of 0.096 m. Below the membrane was a pressurized air chamber. This chamber ensured that the membrane remained in a horizontal position after the outer column was filled with liquid (a necessary condition for the membrane to be properly displaced by the vibrator) by allowing for pressure compensation. Air was fed into the riser column through 11 of 12 stainless-steel capillary gas distributors each with an internal diameter of 0.9 mm; see Fig. 2c. The outlet points on the gas distributors were at height of 0.12 m from bottom of the reactor. The rate of air flow into the reactor was controlled using pre-calibrated rotameters (*Sho-Rate Brooks Instruments BV, The Netherlands*).

An air-cooled vibration exciter (*TIRAvib 5220, TIRA Maschinenbau GmbH, Germany*) was attached to the bottom of the outer column. This vibrator was coupled to a power amplifier. The vibration system was fully automated and controlled from a PC using Signal Calc 550 Vibration Controller software (*Data Physics Corporation, United States*). The vibration exciter has been described fully in earlier publications (Ellenberger and Krishna, 2002, 2003; Krishna and Ellenberger, 2002).

For comparison purposes, experimental studies were also carried out in an airlift loop reactor and a bubble column. The set-up of the airlift loop reactor was a modification of the 35 cpsi monolith reactor in which the monolith tube bundle was removed from the riser column and the length of the riser column extended by 0.099 m. Thus, like the monolith loop reactors, the airlift loop reactor comprised of an outer column, a riser column and a gas–liquid separator unit.

The bubble column, with an internal diameter of 0.1 m and a height of 3.18 m was made of polyacrylate. Like the monolith loop reactors, both the airlift loop reactor and the bubble column were coupled to the vibration control system. All reactor configurations used the same gas distributor device (see Fig. 2c), consisting of 12 stainless-steel capillaries of 0.9 mm inside diameter. Table 1 gives a summary of the principal dimensions of the four reactor column configurations employed in this study and further information on the experimental set-ups including photographs and sample videos on the operation of the monoliths can be found on our website (Vandu et al., 2003).

3. Experimental procedure

Air was used as the gas phase and demineralized water as the liquid phase in all experiments carried out. Measurements were made of the gas holdup and volumetric mass-transfer coefficient in each of the four reactor column configurations described above. Downcomer liquid velocity

Table 1
Dimensions of the reactor configurations employed

	Height of riser column (m)	Inner diameter of riser column (m)	Outer diameter of riser column (m)	Inner diameter of outer column (m)	Height of monolith segments (m)
Monolith loop: square channel	1.57	0.068	0.075	0.1	1.5
Monolith loop: circular channel	1.53	0.069	0.079	0.1	1.47
Airlift lift loop reactor	1.63	0.069	0.079	0.1	—
Bubble column reactor	—	—	—	0.1	—

measurements were also made in the monolith loop reactors as well as in the airlift loop reactor. At the start of each experimental run, the clear liquid height was set at 0.16 m in the gas–liquid separator of the monolith and airlift loop reactors. The clear liquid height in the bubble column was set at 1.18 m above the gas distributor. The monolith and airlift loop reactors were always operated in such a way that no gas bubbles were present in their downcomers.

For every reactor configuration, experiments were first carried out without vibration. This was followed by a corresponding experimental set wherein the vibration control system was utilized. In all vibration experiments, the vibrator was programmed to generate low-frequency sine wave oscillations with an amplitude, λ of 0.5 mm and a frequency, f of 60 Hz; the choice of these vibration parameters were made on the basis of our earlier studies on bubble columns (Ellenberger and Krishna, 2002, 2003; Krishna and Ellenberger, 2002).

3.1. Gas holdup measurements

Gas holdup measurements were made in the riser section of the monolith and the airlift loop reactors using the technique that we had used in an earlier study (Vandu et al., 2004b). In the monolith loop reactors, the riser gas holdup was measured by trapping gas from the monolith channels in a 0.05 m diameter, 0.75 m high measuring cylinder. The measuring cylinder was initially filled with demineralized water using a suction valve located at its top. It was vertically pre-positioned in the gas–liquid separator using clamps and metal rods. At the moment the gas flow into the column was shut, the measuring cylinder was instantaneously displaced to rest above the rise tube. Gas bubbles leaving the riser tube were then trapped in the measuring cylinder, displacing an equivalent volume of liquid. Based on the volume of trapped gas, the riser gas holdup was determined. The gas holdup in the riser section of the airlift loop reactor was measured by sealing the top of its riser column with a pre-calibrated plastic stopper at the moment gas flow into the column was shut down. In this way, gas was trapped in the riser. The height of the trapped gas was read using a graduated rule affixed on the riser tube, from which the volume of gas and thus, the gas holdup were determined. For each gas flow rate in the monolith and airlift loop reactors, the gas holdup experiments were done in triplicate and an average holdup value taken. Gas holdup values in the bubble column were obtained by visual observation. The gas holdup in this case, is defined as:

$$\varepsilon_G = 1 - \frac{H}{H_0}, \tag{1}$$

where H is the dispersion height and H_0 the initial liquid height above the gas distributor.

3.2. Downcomer liquid velocity measurements

Liquid velocity measurements were carried out in the downcomers of the monolith and airlift loop reactors using the salt pulse tracer injection technique described in our earlier work (van Baten et al., 2003) and on our website (Vandu et al., 2003). For each superficial gas velocity, with or without vibration excitement, three liquid velocity measurements were carried out. The average liquid velocity values are reported in this paper.

3.3. Volumetric mass-transfer coefficient measurements

The volumetric mass-transfer coefficient, k_La, was determined by means of a dynamic oxygen absorption technique. An oxygen electrode (*YSI Incorporated Model 5331*) inserted 0.15 m above the base of the outer column was used to measure the change in dissolved oxygen concentration (a measuring point which resides in the downcomer section of the monolith and airlift loop reactors—refer to Fig. 1). Dissolved oxygen was stripped from the liquid phase to a negligible concentration by the use of nitrogen sparged through the gas distributor capillaries. After the stripping operation, a step input of air was introduced into the column, with the uptake of oxygen into the liquid phase continuously monitored by the oxygen sensor. Sufficient time was given in each experimental run for the oxygen saturation concentration in the liquid, C_L^* to be reached. Prior to conducting

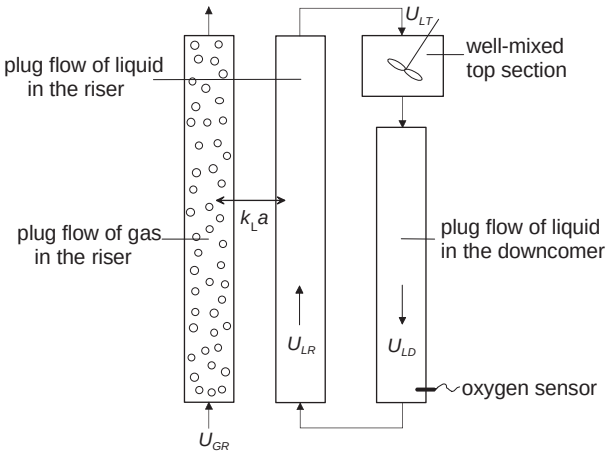

Fig. 3. Schematic representation of the reactor model used to determine k_La in the monolith and airlift loop reactors. For further details of the reactor models visit our website (Vandu et al., 2003).

mass-transfer experiments, the time constant of the oxygen sensor k_{sensor} was determined as described in our earlier work (Vandu and Krishna, 2004) on bubble columns. The membrane surrounding the oxygen electrode was replaced frequently and the sensor constant determined for each membrane. The value of k_{sensor} was found to vary in the range 0.42–0.59 s^{-1} for all experiments carried out. The value of the sensor constant k_{sensor} is about five times higher than the measured k_La values reported later; this means that the sensor dynamics has only a small influence on the k_La values.

A common reactor model was developed for the monolith and airlift loop reactors for obtaining volumetric mass-transfer coefficient values from experimental dynamic oxygen absorption curves based on the following assumptions:

- Plug flow of gas and liquid in the riser section of the reactor.
- Plug flow of liquid in the downcomer section.
- A well-mixed gas–liquid separator section.

The riser section of the reactor is assumed to extend to the dispersion height. This means that gas bubbles in the gas–liquid separator constitute a part of the riser, i.e. no gas bubbles are assumed to be present in the gas–liquid separator. The gas free gas–liquid separator is referred to as the top section in the model developed. A diagram of the model is shown in Fig. 3. The governing mass balance equations for the reactor model are:

Plug flow of gas in the riser:

$$\varepsilon_G \frac{\partial(C_{GR})}{\partial t} = -U_G \frac{\partial\,(C_{GR})}{\partial h} - k_La\left(\frac{C_{GR}}{m} - C_{LR}\right). \quad (2)$$

Plug flow of liquid in the riser:

$$\varepsilon_L \frac{\partial(C_{LR})}{\partial t} = -U_{LR} \frac{\partial(C_{LR})}{\partial h} + k_La\left(\frac{C_{GR}}{m} - C_{LR}\right). \quad (3)$$

Well-mixed top section:

$$\frac{\partial(C_{LT})}{\partial t} = -U_{LT} \frac{\Delta(C_{LT})}{H_T}. \quad (4)$$

Plug flow of liquid in the downcomer:

$$\frac{\partial(C_{LD})}{\partial t} = U_{LD} \frac{\partial(C_{LD})}{\partial h}. \quad (5)$$

Sensor correction equation:

$$\frac{\mathrm{d}(C_{\text{sensor}})}{\mathrm{d}t} = k_{\text{sensor}}(C_{LD} - C_{\text{sensor}}). \quad (6)$$

ε_G and ε_L are the gas and liquid holdups in the *riser section* of the monolith and airlift loop reactors. k_La is the volumetric mass-transfer coefficient per unit volume of *dispersion* (gas + liquid) in the *riser section* of the monolith and airlift loop reactors. U_G is the superficial gas velocity with respect to the riser section of the reactor (based on open area available for flow of gas and liquid phases in case of monolith configurations) while U_{LR}, U_{LT} and U_{LD} are the superficial liquid velocities in the riser, top section and downcomer, respectively. The values of U_{LD} as determined experimentally were used in the reactor model. Figs. 4a–c show the experimentally determined U_{LD} values as a function of U_G for the circular-channel monolith, square-channel monolith and airlift reactors, respectively, with and without the effect of vibration excitement. Note that for a given U_G, columns with larger cross-sectional area available for gas–liquid flow have higher gas flow rates. The increase in U_{LD} with vibration excitement for a given superficial gas velocity is due to an increase in gas holdup in the riser, as we will discuss below which results in an increase in lift-force of the gas bubbles. This lift-force increase yields a higher pressure difference between the top of bottom of the downcomer causing an increase in its liquid velocity. Once U_{LD} is known the U_{LR} and U_{LT} values are determined from geometry considerations, using the known cross-sectional areas. H_T is the dispersion height of the top section and m, the solubility coefficient of oxygen in water; $m = 28$. Eqs. (2)–(6) are subject to the following boundary conditions:

- at time $t = 0$, $C_{GR} = C_{GR,\text{inlet}}$,
- at time $t = 0$, $C_{LR} = C_{LD} = 0$,
- $C_{LR,\text{in}} = C_{LD,\text{out}}$,
- $C_{LD,\text{in}} = C_{LT,\text{out}}$,
- $C_{LT,\text{in}} = C_{LR,\text{out}}$.

Solving the equations involved discretizing their spatial derivates. A first-order backward difference approximation was used. The Method of Lines solution procedure was adopted with 50 grid points used to represent the total dispersion height in the reactor. A FORTRAN program was written to handle this, utilizing the ODE solver LSODE (Hindmarsh, 2001) in double precision. Figs. 5a–c show sample k_La fits, without vibration excitement, in the circular-, square-channel monolith and airlift reactors at

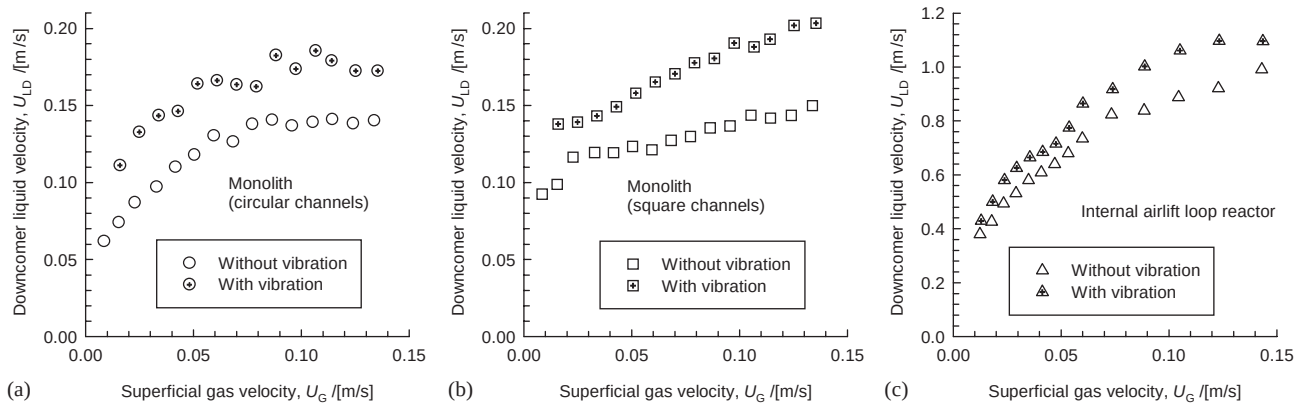

Fig. 4. Variation in measured downcomer liquid velocity, U_{LD} with superficial gas velocity, U_G in the (a) circular-channel monolith loop reactor (b) square-channel monolith loop reactor (c) internal airlift reactor, with and without vibration excitement.

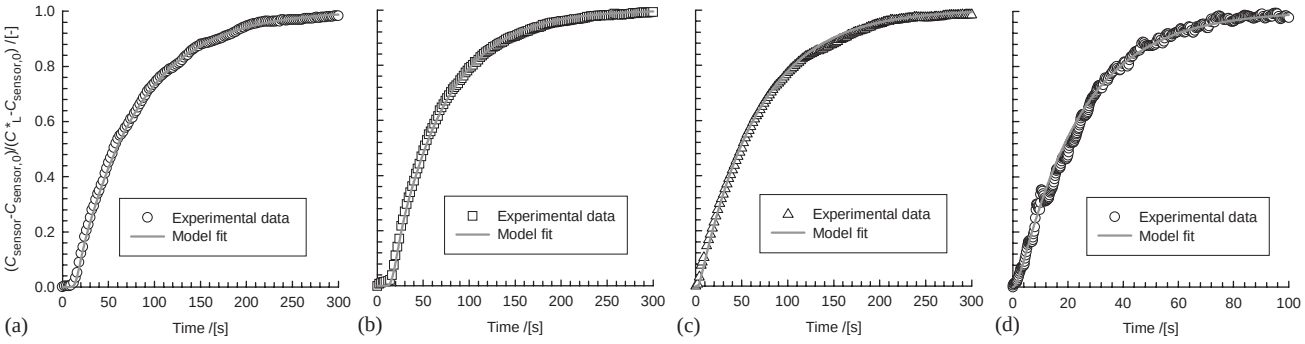

Fig. 5. Oxygen absorption dynamics for the specified superficial gas velocities, U_G in the (a) circular-channel monolith loop reactor (b) square-channel monolith loop reactor (c) internal airlift reactor and (d) bubble column, as well as the reactor model fits obtained for each case in obtaining k_La values.

$U_G = 0.114$, 0.09 and 0.143 m/s, respectively. The k_La values obtained from these fits are 0.127, 0.102 and 0.051 s^{-1}, respectively.

For the determination of the k_La for bubble columns we assumed plug flow of gas and completely mixed liquid phase (details available elsewhere (Vandu et al., 2003; Vandu and Krishna, 2004)). A typical bubble column model fit for obtaining the value of k_La is shown in Fig. 5d. For this case, $U_G = 0.048$ m/s (without vibration excitement) and the k_La value obtained is 0.038 s^{-1}. Further description of the experimental procedure and the models used to determine k_La can be found elsewhere (Vandu et al., 2003).

4. Results and discussions

The measured data on the gas holdup ε_G, volumetric mass-transfer coefficient, k_La, and the ratio k_La/ε_G, as a function of the superficial gas velocity U_G based on the open area available for flow of the phases, for the four reactor configurations investigated, both with and without vibrations, are summarized in Figs. 6a–f. For the monoliths and airlift, the gas holdup refers to the fractional gas holdup in the riser section. For all four reactor configurations vibrations result in a significant improvement in the gas holdup, ε_G and the mass-transfer coefficient, k_La. Our earlier work has shown that low-frequency vibrations have the effect of reducing the rise velocity of the bubble swarm due to the creation of standing waves (Ellenberger and Krishna, 2003) and the influence of the Bjerknes force (Bjerknes, 1906) that acts on the bubbles. Applying vibrations to the monoliths also serves to improve the distribution of gas and liquid in the monolith channels. A froth consisting of tiny bubbles is created just above the gas distributor enhancing the distribution of gas in the monolith channels; this effect is best appreciated by viewing the video recordings (Vandu et al., 2003). Vibrations also improve k_La/ε_G, suggesting that there is also an enhancement in k_L.

The monolith reactors, with either circular or square channels, show a significantly higher value of k_La than conventionally used bubble columns and internal airlift reactor configurations, when the comparison is made at the same U_G. We note that the mass-transfer coefficient per unit volume of dispersed gas bubbles, k_La/ε_G, is about a factor two higher for monoliths than for a conventional bubble column, emphasising the superiority of monoliths for carrying out fast reactions.

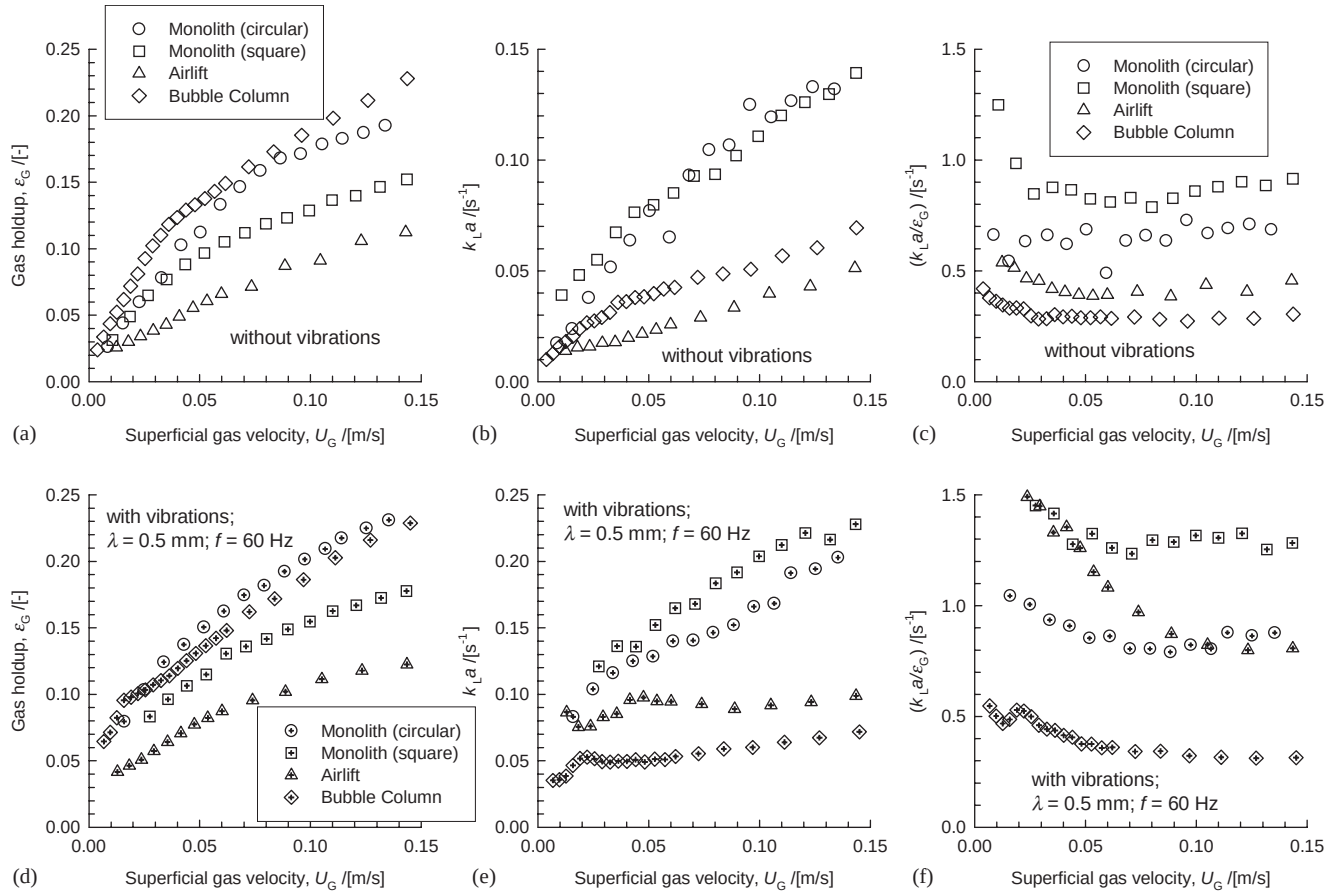

Fig. 6. Influence of variation in superficial gas velocity, U_G on (a) gas holdup, ε_G (b) volumetric mass-transfer coefficient, k_La and (c) k_La/ε_G in each of the four reactor configurations investigated without vibration. Influence of variation in superficial gas velocity, U_G on (d) gas holdup, ε_G (e) volumetric mass-transfer coefficient, k_La and (f) k_La/ε_G for the case with vibration with $\lambda = 0.5$ mm and $f = 60$ Hz. For video recordings of the column operations, with and without vibration, visit our website (Vandu et al., 2003).

In order to understand the holdup and mass-transfer characteristics of circular and square monoliths, we carried out a separate study to determine the unit cell lengths and bubble rise velocities in single capillaries for various U_G and U_{LR} values as encountered in our monolith loop reactors used in this study; these experiments are described elsewhere (Vandu et al., 2004a). Within the channels we have Taylor flow, resulting in a train of bubbles that are separated from one other by liquid slugs (Thulasidas et al., 1995); see Fig. 7a. The bubbles are surrounded by a thin liquid film, that is of the order of 50–200 μm, depending on the gas and liquid superficial velocities, U_G and U_{LR} through each monolith channel (Kreutzer, 2003). The Taylor bubble rise velocity V_b in circular and square capillaries of 3 mm channel dimensions are shown in Fig. 7b. We found that the Taylor bubble rise velocity was 10% higher than the sum of the superficial gas and liquid velocities in the capillaries, $(U_G + U_{LR})$. The relation $V_b = 1.1(U_G + U_{LR})$ provides an accurate estimate of the Taylor bubble rise velocity within the channels. The unit cell length L_{UC} is predominantly determined by the superficial gas velocity; see Fig. 7c.

Knowledge of the Taylor bubble rise velocity and the unit cell length should allow the estimation of the volumetric mass-transfer coefficient following the recently developed mass-transfer model by van Baten and Krishna (2004) using CFD simulations as basis. Their model recognizes two contributions to mass transfer: (1) from the two *hemispherical caps* at either end of the Taylor bubble, and (2) the *film* surrounding the bubble:

$$k_La = k_{L,\mathrm{cap}}a_{\mathrm{cap}} + k_{L,\mathrm{film}}a_{\mathrm{film}} \tag{7}$$

with

$$k_{L,\mathrm{cap}} = 2\sqrt{\frac{2Đ V_b}{\pi^2 d_c}} \tag{8}$$

and

$$k_{L,\mathrm{film}} \approx 2\sqrt{\frac{Đ}{\pi t_{\mathrm{film}}}} \tag{9}$$

where t_{film}, the contact time of the liquid film with the rising Taylor gas bubble, can be estimated as $t_{\mathrm{film}} = L_{UC}\varepsilon_G/V_b$.

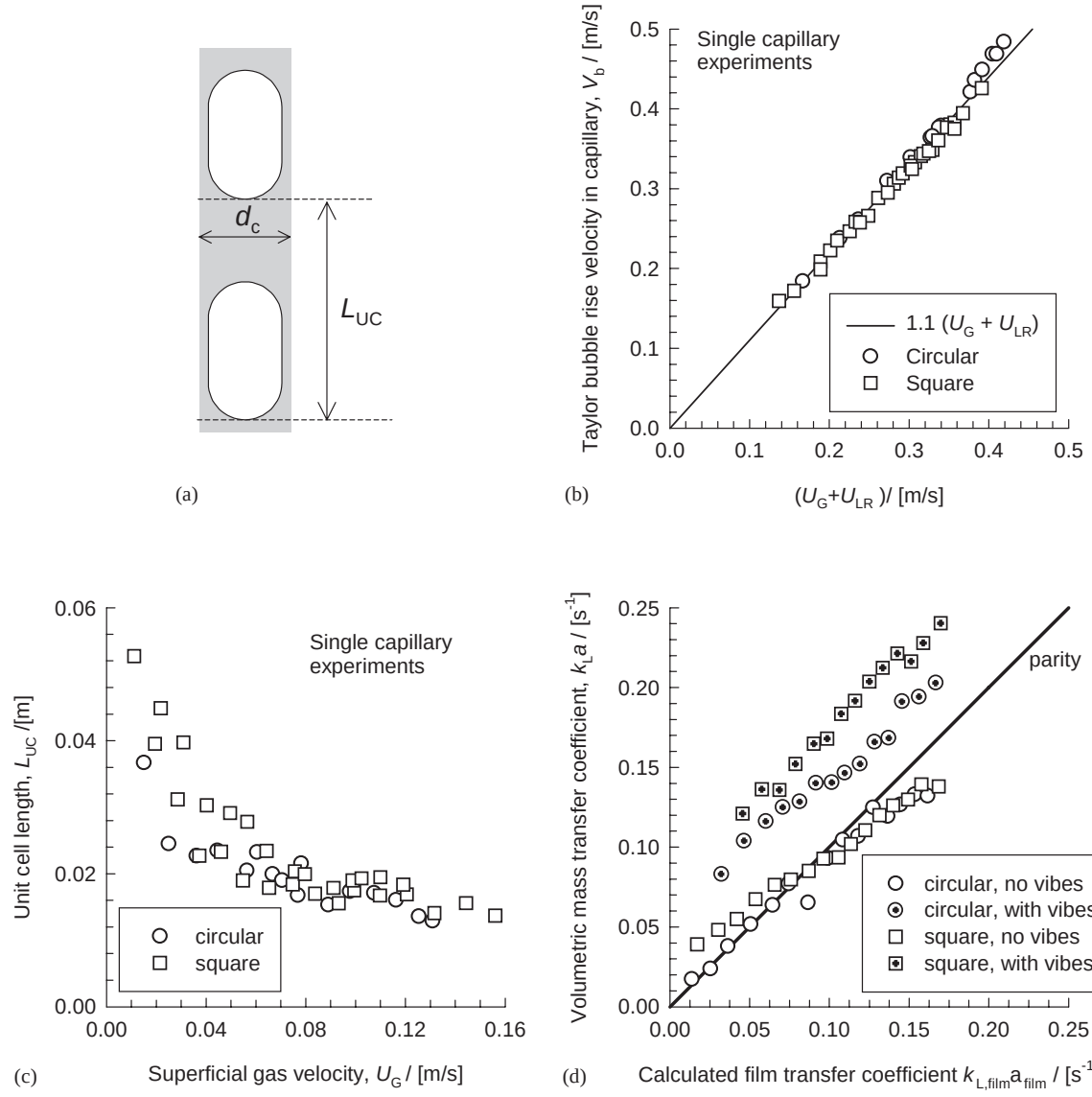

Fig. 7. (a) Schematic of Taylor flow in capillary. (a) Dependence of Taylor bubble rise velocity on $(U_G + U_{LR})$ for circular and square capillaries of 3 mm diameter. (c) Unit cell lengths in 3 mm single capillary of circular and square cross-sections as function of the superficial gas velocity. (d) Comparison of experimentally determined volumetric mass-transfer coefficients k_La in the monolith loop reactor with the predictions using Eqs. (7)–(9). The hydrodynamic data on V_b, and L_{UC} were those obtained from the single-channel experiments. The continuous solid line represents the parity line.

van Baten and Krishna (2004) found that the film contribution to mass transfer was dominant, accounting for about 80% of the transfer from Taylor bubbles. The calculations of the film contribution to k_La values using Eq. (9) along with $a_{film} = 4\varepsilon_G/d_c$ using the V_b and L_{UC} estimations using the single capillary experimental data are shown in Fig. 7d. In the $k_{L,film}a_{film}$ calculations the experimentally determined values of gas holdup in the monoliths were used. For the no-vibrations case in both circular and square capillaries the experimental k_La values agree very well with the film contribution, $k_{L,film}a_{film}$. Calculations using the Bercic and Pintar (1997) correlation yielded k_La predictions that are about a factor 2.5 higher than the experimental values for the no-vibrations case. The reason for this discrepancy is that the Bercic–Pintar correlation was developed using experiments in which very large unit cells, of the order of 0.22 m, were realized. In our experiments, the unit cells were typically in the 0.01–0.06 m range. Application of vibrations has the effect of doubling the value of k_La when compared to the no-vibration case. This enhancement is probably due to enhanced turbulence at the gas–liquid interface and due to better distribution of gas and liquid phases through the channels.

5. Conclusions

The hydrodynamics and mass-transfer characteristics of monolith loop reactors, with upflow of gas and liquid phases

through the channels, have been investigated in this study and compared with conventional internal airlift reactor and bubble column configurations. The following major conclusions can be drawn from this work:

(1) The volumetric mass-transfer coefficient per unit volume of dispersed gas bubbles, k_La/ε_G, is significantly higher for monolith reactors than for airlift and bubble columns. This improvement is due to the superior mass-transfer characteristics of Taylor flow in narrow capillaries.
(2) Application of low-frequency vibrations (with amplitude $\lambda = 0.5$ mm and frequency $f = 60$ Hz) has the effect of significantly improving k_La/ε_G for all four reactor configurations studied. These results are in line with our previous study on the influence of vibrations on bubble column reactor performance (Ellenberger and Krishna, 2002, 2003). For monoliths, vibrations have the beneficial effect of improving the gas–liquid distribution through the channels.
(3) Both gas and liquid superficial velocities within the monolith channels influence the hydrodynamics, i.e. Taylor bubble rise velocity and unit cell length. The knowledge of these parameters is essential to the estimation of the mass-transfer from Taylor bubbles.
(4) The k_La values for monoliths for the no-vibrations case can be estimated with reasonable accuracy using the model developed by van Baten and Krishna (2004), with the additional assumption that the "film" contribution is dominant.

Notation

a	gas–liquid interfacial area per unit volume of dispersion;except for bubble columns the dispersion within the riser section is considered, $m^2\,m^{-3}$
C_{GR}	gas-phase oxygen concentration in the riser, mol/m^3
C_{LD}	liquid-phase oxygen concentration in the downcomer, mol/m^3 or arbitrary units
C_L	liquid-phase oxygen concentration, mol/m^3
C_{LR}	liquid-phase oxygen concentration in the riser, mol/m^3
C_{LT}	liquid-phase oxygen concentration in the gas–liquid separator (top section), mol/m^3
C_{sensor}	liquid-phase oxygen concentration indicated by the sensor, arbitrary units
d_c	capillary channel dimension, m
Đ	liquid-phase diffusivity, m^2/s
f	vibration frequency, Hz
H	total dispersion height, m
H_T	dispersion height in the gas–liquid separator (top section), m
k_L	liquid-side mass-transfer coefficient, m/s
k_{sensor}	sensor time constant, s^{-1}
L_{UC}	length of unit cell, m
m	solubility coefficient of oxygen in water, dimensionless
U_G	superficial gas velocity in the riser, m/s
U_{LD}	downcomer superficial liquid velocity, m/s
U_{LR}	riser superficial liquid velocity, m/s
U_{LT}	top section superficial liquid velocity, m/s
V_b	Taylor bubble rise velocity, m/s

Greek letters

ε_G	riser gas holdup, dimensionless
ε_L	riser liquid holdup, dimensionless
λ	amplitude of vibration, mm

Subscripts and superscripts

cap	refers to hemispherical cap
film	refers to liquid film
G	refers to gas phase
in	refers to conditions into a given section of the reactor
inlet	refers to conditions at the inlet of the reactor
L	refers to liquid phase
0	initial condition
out	refers to conditions out of a given section of the reactor
UC	unit cell
*	refers to saturation concentration

Acknowledgements

Sasol Technology Netherlands BV is gratefully acknowledged for partial financial support and we acknowledge several useful discussions with Dr. B. Breman and Dr. W. Brilman of Sasol. Corning GmbH is gratefully acknowledged for provision of the cordierite square-channel monolith. We also acknowledge useful discussions with Dr. T. Boger of Corning. The Netherlands Foundation for Scientific Research-Chemical Sciences division (NWO-CW) provides a research program subsidy; this was used to purchase the vibration exciter.

References

Bercic, G., Pintar, A., 1997. The role of gas bubbles and liquid slug lengths on mass transport in the Taylor flow through capillaries. Chemical Engineering Science 52, 3709–3719.

Bjerknes, V., 1906. Fields of Force, Columbia University Press, New York.

Boger, T., Roy, S., Heibel, A.K., Borchers, O., 2003. A monolith loop reactor as an attractive alternative to slurry reactors. Catalysis Today 79, 441–451.

Ellenberger, J., Krishna, R., 2002. Improving mass transfer in gas–liquid dispersions by vibration excitement. Chemical Engineering Science 57, 4809–4815.

Ellenberger, J., Krishna, R., 2003. Shaken, not stirred, bubble column reactors: enhancement of mass transfer by vibration excitement. Chemical Engineering Science 58, 705–710.

Heibel, A.K., Scheenen, T.W.J., Heiszwolf, J.J., Van As, H., Kapteijn, F., Moulijn, J.A., 2001. Gas and liquid phase distribution and their effect on reactor performance in the monolith film flow reactor. Chemical Engineering Science 56, 5935–5944.

Heiszwolf, J.J., Engelvaart, L.B., van den Eijnden, M.G., Kreutzer, M.T., Kapteijn, F., Moulijn, J.A., 2001. Hydrodynamic aspects of the monolith loop reactor. Chemical Engineering Science 56, 805–812.

Hindmarsh, A.C., 2001. Livermore Solver for Ordinary Differential Equations. Lawrence Livermore National Laboratory, Livermore, California. http://www.llnl.gov/CASC/.

Kapteijn, F., Nijhuis, T.A., Heiszwolf, J.J., Moulijn, J.A., 2001. New non-traditional multiphase catalytic reactors based on monolithic structures. Catalysis Today 66, 133–144.

Kreutzer, M.T., 2003. Hydrodynamics of Taylor flow in capillaries and monolith reactors. Ph.D. Thesis, Delft University of Technology. Delft, The Netherlands

Krishna, R., Ellenberger, J., 2002. Improving gas–liquid contacting in bubble columns by vibration excitement. International Journal of Multiphase Flow 28, 1223–1234.

Nijhuis, T.A., Kreutzer, M.T., Romijn, A.C.J., Kapteijn, F., Moulijn, J.A., 2001. Monolithic catalysts as efficient three-phase reactors. Chemical Engineering Science 56, 823–829.

Roy, S., Heibel, A.K., Liu, W., Boger, T., 2004. Design of monolithic catalysts for multiphase reactions. Chemical Engineering Science 59, 957–966.

Stankiewicz, A., 2001. Process intensification in in-line monolithic reactor. Chemical Engineering Science 56, 359–364.

Thulasidas, T.C., Abraham, M.A., Cerro, R.L., 1995. Bubble-train flow in capillaries of circular and square cross-section. Chemical Engineering Science 50, 183–199.

van Baten, J.M., Krishna, R., 2004. CFD simulations of mass transfer from Taylor bubbles rising in circular capillaries. Chemical Engineering Science 59, 2535–2545.

van Baten, J.M., Ellenberger, J., Krishna, R., 2003. Hydrodynamics of internal air-lift reactors: experiments vs. CFD simulations. Chemical Engineering and Processing 42, 733–742.

Vandu, C.O., Ellenberger, J., Krishna, R., 2003. Hydrodynamics and mass transfer of monoliths, bubble columns and airlifts (with and without vibration excitement). http://ct-cr4.chem.uva.nl/BubbleColumnAirliftMonolith/, 17 November 2003.

Vandu, C.O., Krishna, R., 2004. Influence of scale on the volumetric mass transfer coefficients in bubble columns. Chemical Engineering and Processing 43, 575–579.

Vandu, C.O., Ellenberger, J., Krishna, R., 2004a. Taylor bubble rise in circular and square capillaries. University of Amsterdam, Amsterdam, The Netherlands. http://ct-cr4.chem.uva.nl/SingleCapillary/, 16 January 2004.

Vandu, C.O., Ellenberger, J., Krishna, R., 2004b. Hydrodynamics and mass transfer in an upflow monolith loop reactor. Chemical Engineering and Processing, in press.